Title

Crk Adaptor Proteins Regulate NK Cell Expansion and Differentiation during Mouse Cytomegalovirus Infection

Journal

The Journal of Immunology, 200(10)

ISSN

0022-1767

Authors

Nabekura, Tsukasa
Chen, Zhiying
Schroeder, Casey
et al.

Publication Date

2018-05-15

DOI

10.4049/jimmunol.1701639

Peer reviewed

The Journal of Immunology

Crk Adaptor Proteins Regulate NK Cell Expansion and Differentiation during Mouse Cytomegalovirus Infection

Tsukasa Nabekura, Zhiying Chen, Casey Schroeder, Taeju Park, Eric Vivier, Lewis L. Lanier and Dongfang Liu

J Immunol 2018; 200:3420-3428; Prepublished online 4 April 2018;
doi: 10.4049/jimmunol.1701639
http://www.jimmunol.org/content/200/10/3420

The Journal of Immunology is published twice each month by
The American Association of Immunologists, Inc.,
1451 Rockville Pike, Suite 650, Rockville, MD 20852

Print ISSN: 0022-1767 Online ISSN: 1550-6606.

Crk Adaptor Proteins Regulate NK Cell Expansion and Differentiation during Mouse Cytomegalovirus Infection

Tsukasa Nabekura,[*,†,‡] Zhiying Chen,[§] Casey Schroeder,[§] Taeju Park,[¶] Eric Vivier,[‖,#] Lewis L. Lanier,[*,†] and Dongfang Liu[§,]**

Natural killer cells are critical in the immune response to infection and malignancy. Prior studies have demonstrated that Crk family proteins can influence cell apoptosis, proliferation, and cell transformation. In this study, we investigated the role of Crk family proteins in mouse NK cell differentiation and host defense using a mouse CMV infection model. The number of NK cells, maturational state, and the majority of the NKR repertoire was similar in Crk x Crk-like (CrkL)–double-deficient and wild type NK cells. However, Crk family proteins were required for optimal activation, IFN-γ production, expansion, and differentiation of Ly49H$^+$ NK cells, as well as host defense during mouse CMV infection. The diminished function of Crk x CrkL–double-deficient NK cells correlated with decreased phosphorylation of STAT4 and STAT1 in response to IL-12 and IFN-α stimulation, respectively. Together, our findings analyzing NK cell–specific Crk-deficient mice provide insights into the role of Crk family proteins in NK cell function and host defense. ***The Journal of Immunology*****, 2018, 200: 3420–3428.**

Natural killer cells play a critical role in host defense against microbial pathogens and cancer (1, 2). NK cells kill target cells by the polarized release of lytic granules through a specialized region of cell–cell contact known as the immunological synapse (IS) (3, 4). Through previous studies of the cytotoxic (5) and inhibitory (6) IS in human NK cells, we discovered that Crk plays an essential upstream role at the IS, influencing signaling events required for both activation and inhibition (7). The molecular mechanisms underlying this dual role, however, remain undefined.

The Crk family of proteins comprises ubiquitously expressed adaptor molecules that are critical to many cellular processes (8, 9). To date, most work has focused on Crk's role in cell apoptosis (10), proliferation (8, 11), and transformation (8); little is known about Crk's role in NK cell function (7). The Crk family of proteins includes CrkI, CrkII (hereafter referred to as Crk), and Crk-like (CrkL), the predominant form of Crk family proteins in NK cells (Y.-H. Hsu, Y. Yang, Z. Chen, and D. Liu, unpublished observations). Crk and CrkL proteins (encoded by two different genes) contain one Src homology (SH) 2 domain and two SH3 domains: N-terminal SH3 domain and C-terminal SH3 domain. CrkI is an alternately spliced form of Crk that contains one SH2 and one SH3 domain but lacks the regulatory phosphorylation site and C-terminal SH3 domain of Crk. During human NK cell activation, the majority of Crk is nonphosphorylated (7, 12). In this nonphosphorylated state, Crk family proteins contribute to cytotoxicity signaling for adhesion, granule polarization, and degranulation (13, 14).

DiGeorge syndrome (DGS) is a primary immunodeficiency originally characterized by abnormal T cell production, severely diminished thymic size (15), and impaired immune cell functions caused by deletions on chromosome 22q11 (16–18), which contains three genes (*TBX1*, *CRKL*, and *ERK2*) that have been investigated to explain the phenotypic features of the human DGS immunodeficiency (19–23).

Crkl$^{-/-}$ mice show phenotype characteristics similar to those of human DGS (21, 22, 24), highlighting the importance of *CRKL* (19–23). Previous studies reported decreased expression of *CRKL* in NK cells and T cells from partial DGS patients (14, 25). However, Tbx1 and Erk2 protein expression levels were comparable

*Department of Microbiology and Immunology, University of California, San Francisco, San Francisco, CA 94143; †Parker Institute for Cancer Immunotherapy, San Francisco, CA 94143; ‡Life Science Center, Tsukuba Advanced Research Alliance, University of Tsukuba, Ibaraki 305-8577, Japan; §Center for Inflammation and Epigenetics, Houston Methodist Research Institute, Houston, TX 77030; ¶Children's Research Institute, Children's Mercy Kansas City, Kansas City, MO 64108; ‖Centre d'Immunologie de Marseille-Luminy, Aix Marseille Université, INSERM, CNRS, 13288 Marseille, France; #Service d'Immunologie, Hôpital de la Timone, Assistance Publique-Hôpitaux de Marseille, 13288 Marseille, France; and **Department of Microbiology and Immunology, Weill Cornell Medical College, Cornell University, New York, NY 10065

ORCIDs: 0000-0002-8386-3607 (T.N.); 0000-0003-3897-3994 (T.P.); 0000-0001-7022-8287 (E.V.); 0000-0003-1308-3952 (L.L.L.).

Received for publication November 28, 2017. Accepted for publication March 13, 2018.

This work was supported in part by National Heart, Lung, and Blood Institute/National Institutes of Health Grant HL125018 and National Institute of Allergy and Infectious Diseases/National Institutes of Health Grants AI124769, AI129594, and AI130197 (all to D.L.) and AI068129 (to L.L.L.), a Houston Methodist Career Cornerstone Award (to D.L.), Baylor–University of Texas Houston Center for AIDS Research Core Support Grant AI036211 from the National Institute of Allergy and Infectious Diseases (to D.L.), a Houston Methodist Research Institute for Academic Medicine National Institutes of Health Competitiveness Initiative Award (to D.L.), the Caroline Weiss Law Fund for Research in Molecular Medicine (to D.L.), the Texas Children's Hospital Pediatrics Pilot Research Fund (to D.L.), and the Lymphoma Specialized Program of Research Excellence Developmental Research Program from Baylor College of Medicine and the Methodist Research Institute (P50 CA126752). L.L.L. is an American Cancer Society professor and is funded in part by the Parker Institute for Cancer Immunotherapy. T.N. is supported by the Friends of Leukemia Research Fund and the Nakajima Foundation. The laboratory of E.V. is supported by the European Research Council (ERC-2015-AdG - 694502_TILC), the Ligue Nationale contre le Cancer (Equipe Labellisée), Innate-Pharma, MSDAvenir, and by institutional grants from INSERM, CNRS, Aix-Marseille University, and Marseille Immunopole to Centre d'Immunologie de Marseille-Luminy.

Address correspondence and reprint requests to Prof. Lewis L. Lanier or Dr. Dongfang Liu, Department of Microbiology and Immunology, University of California, San Francisco, 513 Parnassus Avenue, Room HSE-1001G, San Francisco, CA 94143-0414 (L.L.L.) or Houston Methodist Research Institute, 6670 Bertner Avenue, R9-216, Houston, TX 77030 (D.L.). E-mail addresses: Lewis.Lanier@ucsf.edu (L.L.L.) or dliu2@houstonmethodist.org (D.L.)

The online version of this article contains supplemental material.

Abbreviations used in this article: BM, bone marrow; BV, Brilliant Violet; CrkL, Crk-like; DGS, DiGeorge syndrome; dKO, double-deficient knockout; IS, immunological synapse; MCMV, mouse CMV; PB, Pacific Blue; pi, postinfection; SH, Src homology; UCSF, University of California, San Francisco; WT, wild type.

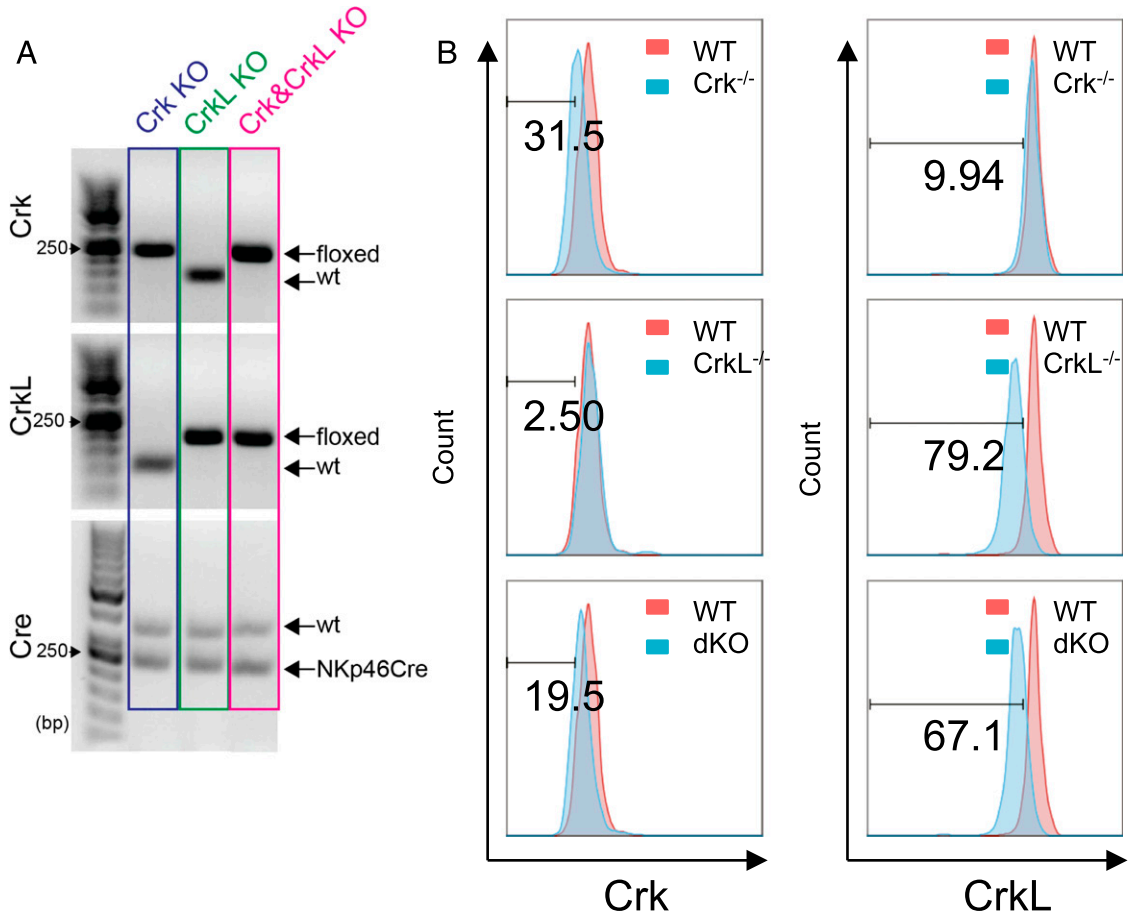

FIGURE 1. Genotype and expression of Crk family proteins in NK cell–specific Crk and CrkL and Crk- and CrkL-dKO NK cells. (**A**) Agarose gel electrophoresis of PCR-amplified DNA extracted from the tail tissue of NKp46-Crk–single-deficient, NKp46-CrkL–single-deficient, and NKp46–Crk-CrkL–dKO mice. PCR products were imaged on a gel documentation system. (**B**) Crk family protein expression revealed by the anti-Crk (clone B-4, left) and anti-CrkL (clone B-1, right) Ab staining is shown on gated NK1.1$^+$NKp46$^+$CD3$^-$ NK cells prepared from the two spleens of NKp46-specific Crk- and CrkL-deficient mice for each experiment. The Crk–single-deficient, CrkL–single-deficient, and dKO (blue) and WT (red) NK cells are compared. Results are representative of three experiments.

to those of NK cells in healthy individuals, indicating the importance of CrkL protein in human NK cells (14). Interestingly, partial DGS patients also have significantly fewer CD27$^+$IgM$^+$IgD$^+$ memory B lymphocytes, suggesting a role for Crk in B cell memory (26–28), which indicates a potential role of Crk family proteins in immune cell memory.

In this study, in a mouse model, we investigated whether Crk family proteins play a similar role in the development of NK cell activation and differentiation, as well as in NK cell defense against viral infection. Specifically, leveraging novel NK cell–specific Crk knockout mice, we investigated Crk's role in NK cell–mediated immune responses to mouse CMV (MCMV) infection.

Materials and Methods

Mice

Congenic CD45.1$^+$ wild type (WT) C57BL/6 (B6) mice were purchased from the National Cancer Institute. Ly49H-deficient (*Klra8*$^{-/-}$) B6 mice (kindly provided by Dr. S. Vidal) (29) and DAP12-deficient (*Tyrobp*$^{-/-}$) mice were maintained at the University of California, San Francisco (UCSF) in accordance with Institutional Animal Care and Use Committee guidelines. NK cell–specific Crk– and CrkL–double-deficient knockout (dKO) B6 mice were generated by crossing Ncr1^{iCre} mice (30) with *Crk*-floxed mice and *Crkl*-floxed mice (31, 32) and were maintained at the Houston Methodist Research Institute in accordance with Institutional Animal Care and Use Committee guidelines. We generated the Crk and CrkL dKO mice as follows: the 129/SvEv embryonic stem cells with floxed *Crk* and *Crkl* genes were injected into B6 mouse blastocysts to generate the Crk- and CrkL-floxed mice (generated at the St. Jude Children's Research Hospital). The mouse lines were maintained on a mixed background of C57BL/6 and 129/SvEv (31). The Crk– and CrkL–single-floxed mice were transferred to the Children's Hospital of Philadelphia and interbred to generate the Crk– and CrkL–double-floxed mice, which were maintained on a mixed background of C57BL/6 and 129/SvEv (32). Then, the Crk– and CrkL–double-floxed mice were transferred to Baylor College of Medicine. The chimeric offspring mice were bred with C57BL/6 mice for at least 10 generations at Baylor College of Medicine. Then, the offspring mice were bred to each other for at least 20 generations. Ncr1^{iCre} C57BL/6 mice, rederivation in B6 mice, were crossed with the Crk- and CrkL-floxed mice to generate the NKp46-specific Crk- and CrkL-dKO mice. Once dKO offspring mice with the desired genotype were identified and validated, they were bred with each other for at least 20 generations. Mixed bone marrow (BM) chimeric mice were generated as described (33). Briefly, BM from CD45.1$^+$CD45.2$^+$ WT B6 mice was mixed 1:1 with BM from CD45.1$^-$CD45.2$^+$ Crk- and CrkL-dKO B6 mice and then injected into lethally irradiated recipient CD45.1$^+$CD45.2$^-$ B6 mice. Hematopoietic cells were allowed to reconstitute for 4–5 wk. BM chimeric mice allow direct comparison of WT and Crk dKO NK cell development and participation in long-term immune responses in a physiological setting (34). Our design uses congenic mouse strains that differ at the CD45 locus. CD45 is expressed by all nucleated leukocytes, allowing donor cells to be easily distinguished, isolated, and assayed (35). In this design, WT (CD45.1$^+$) and Crk$^{-/-}$ dKO (CD45.1$^-$) NK cells developed in the same environment, dramatically minimizing environmental variants.

NK cell enrichment, adoptive transfer, and MCMV infection

NK cells were enriched from splenocytes from mixed BM chimeric mice 4 wk or later after BM transplantation using Qiagen BioMag goat anti-rat IgG magnetic beads (catalog no. 310107) (36). Briefly, splenocytes were

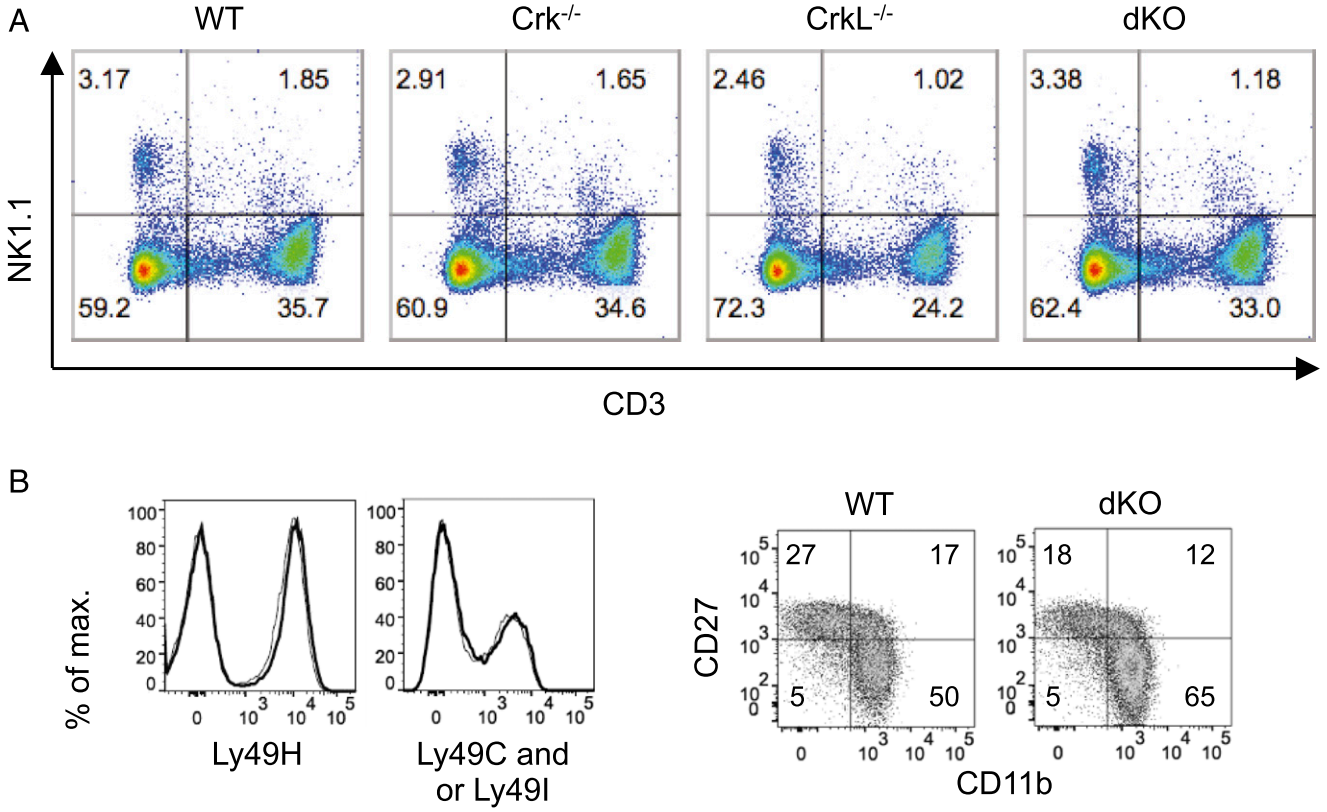

FIGURE 2. NK cells in Crk, CrkL, and Crk- and CrkL-dKO mice. (**A**) Percentages of splenic NK cells (gated on $CD3^-$ and $NK1.1^+$) in NKp46-Crk–single-deficient, NKp46-CrkL–single-deficient, and NKp46–Crk-CrkL dKO mice. Data are representative of analysis of two independent experiments from 8-wk sex-matched mice. The numbers of total splenocytes harvested from these three genotypes of mice were comparable. (**B**) Expression of Ly49H, Ly49CR, and Ly49IR (left) and the developmental stages, as determined by expression of CD11b and CD27 (right) on WT (bold lines) and dKO (thin lines) NK cells, gating on $TCR\beta^-NK1.1^+$ lymphocytes in the spleens of mixed BM chimeric mice. Data are representative of two to four experiments (n = 2–7 mice per experiment).

incubated with 5 μg purified rat mAbs obtained from the UCSF mAb Core against mouse CD4 (GK1.5), CD5 (53-7.3), CD8 (2.43), CD19 (1D3), Gr-1 (RB6-8C5), and Ter119, followed by anti-rat IgG beads (Qiagen BioMag). In some assays, mouse NK cells were purified by using Miltenyi Mouse NK Cell Isolation Kit II (catalog no. 130-096-892; Miltenyi Biotec).

For adoptive transfer, 3×10^5 $Ly49H^+$ NK cells were injected i.v. into Ly49H-deficient B6 mice 24 h prior to infection by i.p. injection with 1–10 $\times$ 10^5 PFU Smith strain MCMV prepared in B6 3T3 cells (37). In certain experiments, 1.5×10^7 splenocytes were labeled with 10 μM CellTrace Violet (Invitrogen) before i.v. injection of adoptively transferred NK cells.

MCMV load

WT and dKO NK cells were sorted (FACSAria III; BD Biosciences) from the spleens of mixed BM chimeric mice, and 3.5×10^4 $Ly49H^+$ NK cells were transferred separately into Ly49H-deficient or DAP12-deficient mice and infected with 1×10^5 PFU MCMV. The copy number of MCMV IE1 gene in DNA prepared from peripheral blood on day 3 postinfection (pi) was determined by quantitative PCR (36, 38).

Flow cytometry

Fc receptors were blocked with 2.4G2 mAb (UCSF mAb Core) before staining with the indicated mAbs or isotype-matched control Abs (BD Biosciences, eBioscience, BioLegend, or Tonbo Biosciences). Abs used were FITC-conjugated anti-mouse 2B4 [clone m2B4 (B6)458.1], FITC-conjugated anti-mouse CD25 (clone PC61), FITC-conjugated anti-mouse CD45.1 (clone A20), FITC-conjugated anti-mouse CD69 (clone H1.2F3), FITC-conjugated anti-mouse CD122 (clone TM-β1), FITC-conjugated anti-mouse Ly49D (clone 4E5), FITC-conjugated anti-mouse Ly49H (clone 3D10), PE-conjugated anti-mouse CD27 (clone LG.3A10), PE-conjugated anti-mouse CD45.2 (clone 104), PE-conjugated anti-mouse CD48 (clone HM48-1), PE-conjugated anti-mouse CD132 (clone TUGm2), PE-conjugated anti-mouse KLRG1 (clone 2F1), PE-conjugated anti-mouse Ly49H (clone 3D10), PE-conjugated anti-mouse NKG2D (clone CX5), PE-conjugated anti-mouse PD-1 (clone J43), PE-conjugated anti-mouse TCR-β (clone H57-597), PerCPCy5.5-conjugated anti-mouse CD27 (clone LG.3A10), PerCPCy5.5-conjugated anti-mouse NK1.1 (PK136), APC-conjugated anti-mouse CD127 (clone A7R34), APC-conjugated anti-mouse IFN-αR1 (clone 1G10), APC-conjugated anti-mouse IFN-γ (clone XMG1.2), APC-conjugated anti-mouse KLRG1 (clone 2F1), APC-conjugated anti-mouse NK1.1 (clone PK136), Alexa Fluor 647–conjugated anti-mouse IL-18Rα (clone BG/IL18RA), APC-conjugated anti-mouse TIGIT (clone 1G9), Alexa Fluor 700–conjugated anti-mouse CD45.1 (clone A20), Alexa Fluor 700–conjugated anti-mouse granzyme B (clone GB11), Alexa Fluor 700–conjugated anti-mouse Ly6C (clone HK1.4), PECy7-conjugated anti-mouse Ly6C (clone AL-21), PECy7-conjugated anti-mouse B220 (clone RA3-6B2), PECy7-conjugated anti-mouse CD49b (clone DX5), PECy7-conjugated anti-mouse TCR-β (clone H57-597), Pacific Blue (PB)–conjugated anti-mouse B220 (clone RA3-6B2), PB-conjugated anti-mouse CD11b (clone M1/70), PB-conjugated anti-mouse CD69 (clone H1.2F3), PB-conjugated anti-mouse Ly49A (clone YE1/48.10.6), PB-conjugated anti-mouse Sca-1 (clone D7), Brilliant Violet (BV) 605–conjugated anti-mouse CD45.1 (clone A20), BV711-conjugated anti-mouse NK1.1 (clone PK136), PECy5-conjugated anti-mouse CD3 (clone 145-2C11), biotinylated anti-mouse CD2 (clone RM2-5), biotinylated anti-mouse CD45.1 (clone A20), biotinylated anti-mouse IFN-γR (clone 2E2), biotinylated anti-mouse KLRG1(clone 2F1), biotinylated anti-mouse Ly49C and or Ly49I (clone 5E6), biotinylated anti-mouse DNAM-1 (clone TX42.1), and BV605-conjugated streptavidin. The Abs used for Crk (clone B-4, SC-390132) and CrkL (clone B-1, SC-365092) detection were purchased from Santa Cruz Biotechnology.

For measuring apoptosis, cells were stained with Alexa Fluor 647–conjugated annexin V (BioLegend). We assessed cell division by staining with Alexa Fluor 647–conjugated anti-Ki67 (clone B56; BD Biosciences). Samples were acquired on either an LSR II or FACSCalibur (BD Biosciences), and data were analyzed with FlowJo software (FlowJo).

Ex vivo stimulation of NK cells

Splenocytes (1×10^6) from mixed WT and dKO BM chimeric mice were incubated in 96-well tissue culture plates coated with anti-NK1.1 (PK136)

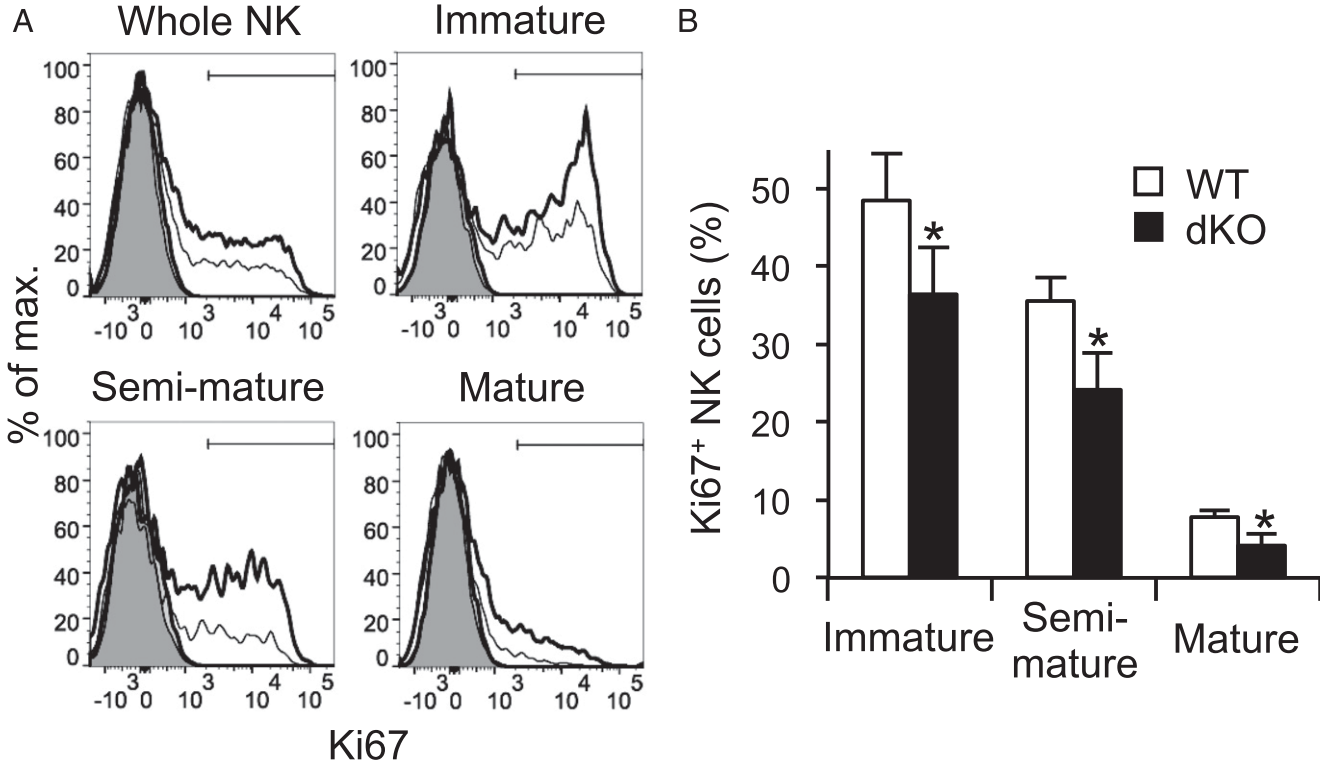

FIGURE 3. Phenotype of dKO NK cells. (**A**) Expression of Ki67 by WT (bold) and dKO (thin lines) on total, immature ($CD11b^{-}CD27^{+}$), semimature ($CD11b^{+}CD27^{+}$), and mature ($CD11b^{+}CD27^{-}$) NK cells in the spleen of BM chimeric mice. Filled and open histograms represent staining with isotype-matched control Ig and anti-Ki67 mAb, respectively. Data are representative of two experiments (n = 3–4 mice per experiment). (**B**) Percentages of $Ki67^{+}$ NK cells. Data were pooled from two experiments (n = 7 mice). *$p < 0.005$ versus WT.

or control mouse IgG2a (39). For cytokine response testing, 1×10^6 splenocytes from mixed WT and dKO BM chimeric mice were incubated with 2.5 ng/ml mouse IL-12 and 2.5 ng/ml mouse IL-18 (R&D Systems). To test degranulation, 1×10^6 splenocytes from mixed WT and dKO BM chimeric mice were cocultured with either 1×10^5 untransfected or m157-transfected B6 3T3 cells for 5 h at 37°C with PE-conjugated anti-CD107a (clone 1D4B) and GolgiStop (BD Biosciences), followed by staining for surface molecules and intracellular IFN-γ. For assessment of phosphorylated STAT4 and p-STAT1, $1–3 \times 10^6$ splenocytes were cultured with 20 ng/ml mouse IL-12 for 30 min or 1000 U/ml mouse IFN-α (PBL Assay Science) for 10 min, fixed, and stained with Alexa Fluor 647–conjugated phosphorylated STAT4 (pY693, clone 38/p-Stat4) or PE-conjugated phosphorylated STAT1 (pY701, clone 4a) (BD Biosciences) (40).

Statistical methods

Student t test (for functional assays) and Mann–Whitney U test (for viral titers) were used. A p value < 0.05 was considered statistically significant. Error bars show SD.

Results

Crk- and CrkL-deficient NK cells

To avoid the embryonic lethal phenotype of *Crk* null mice (22, 31) and potential redundancy between Crk and CrkL, we generated NK cell–specific $Crk^{-/-}$ x $Crkl^{-/-}$ dKO mice by crossing NKp46-Cre knockin mice (30) with *Crk*-floxed x *Crkl*-floxed mice (32). Genotype and flow cytometric analysis confirmed successful generation of three classes of NK cell–specific Crk knockout, CrkL knockout, and Crk x CrkL dKO mice (Fig. 1). The percentages of splenic NK cells ($CD3^{-}NK1.1^{+}$) among WT, NKp46-Crk–single-deficient, NKp46-CrkL–single-deficient, and NKp46–Crk-CrkL dKO mice were comparable (Fig. 2A). To directly compare the role of Crk in NK cells, WT and dKO BM chimeric mice were generated by transferring a 1:1 mixture of $CD45.1^{+}CD45.2^{+}$ WT and $CD45.1^{-}CD45.2^{+}$ dKO B6 BM cells into lethally irradiated $CD45.1^{+}$ $CD45.2^{-}$ B6 recipients. Analysis of WT and dKO NK cells in the BM chimeric mice revealed no substantial differences in the expression of CD2, CD48, Ly49A, Ly6C, CD49b, NK1.1, NKG2D, CD25, CD122, CD127, CD132, IFN-γR, IFN-αR1, B220, PD-1, CD69, DNAM-1, TIGIT, IL-18R-α, or Sca-1 (data not shown), or in Ly49H and Ly49C/I (Fig. 2B, left). The frequency (65%) of mature dKO NK cells ($CD27^{-}$ $CD11b^{+}$) was slightly higher than WT (50%) (Fig. 2B, right). A similar trend was observed in blood, spleen, liver, and BM (data not shown), indicating that dKO NK cells have slightly more mature NK cells. A lower frequency of recently divided $Ki67^{+}$ cells was observed in dKO NK cells when compared with WT NK cells in the BM chimeric mice (Fig. 3). Overall, the number, maturational state, and NKR repertoire of dKO and WT NK cells were similar.

dKO NK cells show defects in degranulation and IFN-γ production

To investigate the functional response to activating receptor– or cytokine-induced activation, WT and dKO NK cells from BM chimeric mice were stimulated with m157-transduced 3T3 cells (41), anti-NK1.1, or IL-12 and IL-18 (Fig. 4). The dKO NK cells exhibited lower levels of m157-induced and anti-NK1.1–induced degranulation (CD107a) and IFN-γ production compared with WT NK cells (Fig. 4A). Similar results were obtained from licensed ($Ly49C/I^{+}$) and unlicensed ($Ly49C/I^{-}$) NK cells (Fig. 4B).

To further evaluate responsiveness of the dKO NK cells to cytokine-induced activation, we investigated the levels of p-STAT4 and p-STAT1 in WT and dKO NK cells from BM chimeric mice cultured with IL-12 or IFN-α, respectively. Compared with WT NK cells, p-STAT1 and p-STAT4 in dKO NK cells were reduced (Fig. 4C–F). Thus, dKO NK cells had diminished degranulation, IFN-γ production, and response to IL-12 and IFN-α compared with WT NK cells that developed in the same host.

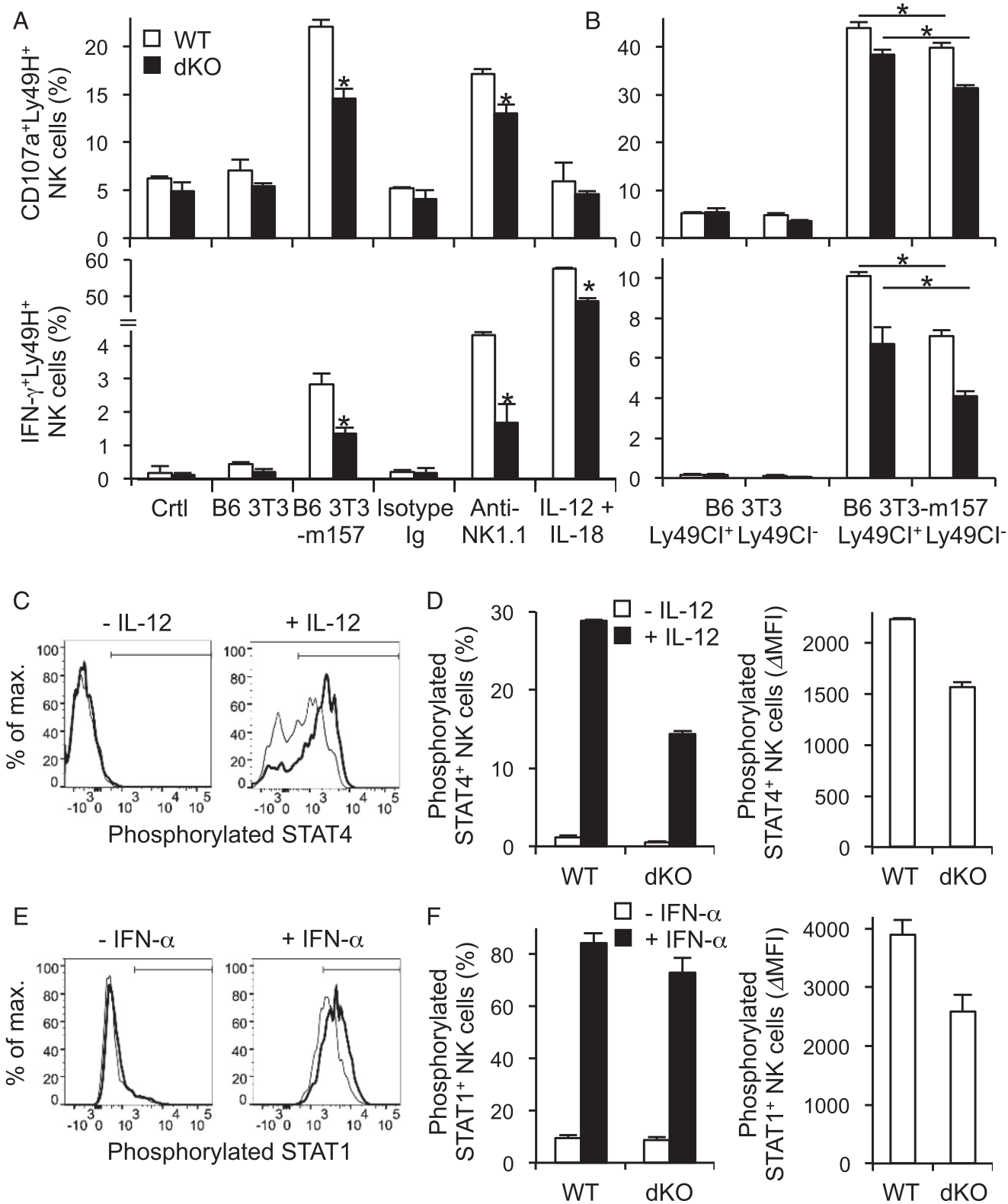

FIGURE 4. Crk proteins affect effector functions of NK cells. (**A**) Degranulation and IFN-γ production of WT (open) and dKO (filled) Ly49H$^+$ NK cells isolated from BM chimeric mice stimulated with m157-transduced 3T3 cells, anti-NK1.1, or IL-12 and IL-18. Data are representative of two to three experiments (n = 3–4 in each stimulation). *$p < 0.05$ versus WT. (**B**) Degranulation and IFN-γ production of WT (open) and dKO (filled) licensed Ly49H$^+$ Ly49C/I$^+$ and unlicensed Ly49H$^+$Ly49C/I$^-$ NK cells stimulated with m157-transduced 3T3 cells. Data are representative of two experiments (n = 3–4 in each stimulation). *$p < 0.05$. (**C**–**F**) Splenocytes from mixed BM chimeric mice were stimulated with 20 ng/ml IL-12 for 30 min (C and D) or 1000 U/ml IFN-α for 10 min (E and F). Phosphorylated STAT4 and p-STAT1 in WT (bold) and dKO (thin lines) were analyzed by intracellular staining (C and E). Percentages of phosphorylated STAT4$^+$ and STAT1$^+$ NK cells and Δ mean fluorescence intensity (ΔMFI), which were calculated by the MFIs of phosphorylated STAT4 and STAT1 after IL-12 and IFN-α stimulation minus MFIs of unstimulated cells (D and F). Data are representative of two experiments (n = 2 in each stimulation).

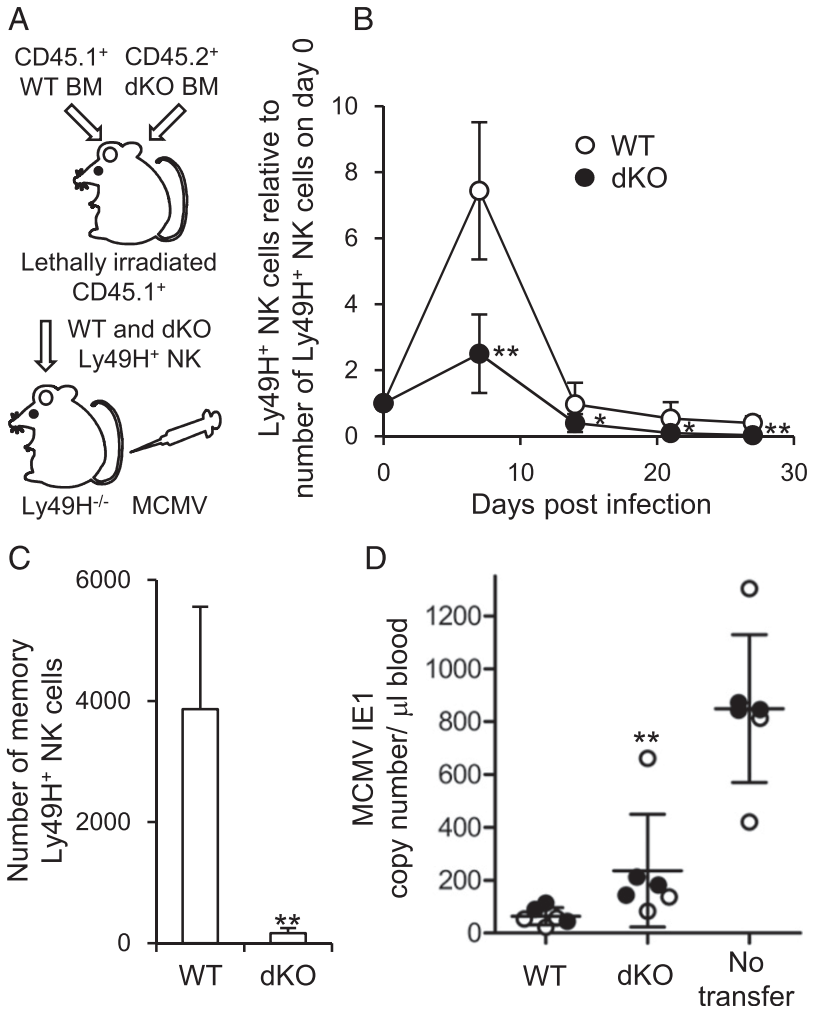

FIGURE 5. Crk proteins are required for optimal expansion of NK cells during MCMV infection. (**A**) WT and dKO Ly49H$^+$ NK cells (3×10^5) purified from mixed BM chimeric mice were transferred into Ly49H-deficient mice and infected with 1×10^5 PFU MCMV. (**B**) The kinetics of the absolute number of Ly49H$^+$ NK cells in the blood were represented as the ratio relative to the number of Ly49H$^+$ NK cells in the blood on day 0. (**C**) The number of memory Ly49H$^+$ NK cells (identified as KLRG1^{high}) in the spleen on day 28 pi. Data were pooled from three experiments ($n = 8$ mice). (**D**) WT and dKO Ly49H$^+$ NK cells (3.5×10^4) sorted from spleens of BM chimeric mice were transferred separately into Ly49H-deficient (open circles) or DAP12-deficient mice (closed circles) and infected with MCMV. Ly49H-deficient or DAP12-deficient mice without transfer of Ly49H$^+$ NK cells (no transfer) were infected with MCMV. The copy number of MCMV IE1 gene in the blood on day 3 pi was analyzed by quantitative PCR. Data were pooled from two experiments ($n = 6$ mice per group). $^*p < 0.05$, $^{**}p < 0.005$ versus WT.

Crk is required for optimal expansion of Ly49H$^+$ NK cells during MCMV infection

In response to MCMV, Ly49H$^+$ NK cells undergo robust expansion to generate long-lived memory NK cells (33, 40). To examine dKO NK cells, we transplanted lethally irradiated recipient mice with CD45.1$^+$ WT and CD45.2$^+$ dKO BM cells and allowed NK cells to reconstitute for 5 wk. NK cells were isolated from BM chimeras, and WT and dKO Ly49H$^+$ NK cells were adoptively transferred into Ly49H-deficient mice. After 24 h, the mice were infected with MCMV (Fig. 5A). The dKO Ly49H$^+$ NK cells showed severe defects in expansion on day 7 pi, and the generation of memory NK cells at 1 mo was significantly decreased (Fig. 5B, 5C). To rule out effects of NK cell trafficking on the generation of memory NK cells, we compared the adhesion and migration molecules (e.g., LFA-1, CCR5, and CXCR3) known to be important between WT and dKO NK cells. The expression of LFA-1, CCR5, and CXCR3 between WT- and Crk-deficient, CrkL-deficient, and Crk- and CrkL-dKO mice was comparable (Supplemental Fig. 1). Furthermore, dKO Ly49H$^+$ NK cells showed an impaired ability to protect against MCMV (Fig. 5D). Thus, the differences in the number of WT and Crk- and CrkL-dKO Ly49H$^+$ NK cells on day 7 pi do not appear to be due to different trafficking of the NK cells.

During MCMV infection, we compared IFN-γ production and granzyme B expression on day 1.5 pi and upregulation of the activation markers CD69 on day 1.5 and KLRG1 on day 7 pi. In the early course of infection, dKO Ly49H$^+$ NK cells produced less IFN-γ and granzyme B and were less activated than WT Ly49H$^+$ NK cells (Fig. 6A). To test whether the lower number of dKO Ly49H$^+$ NK cells generated after infection was due to a higher frequency of cell death and/or lower proliferation, CellTrace Violet–labeled splenocytes from BM chimeric mice were transferred into Ly49H-deficient mice and infected with MCMV. No significant difference in the percentages of annexin V$^+$ cells was observed between WT and dKO NK cells on day 4 pi (Fig. 6B, 6C). We observed a significantly smaller percentage of dividing dKO Ly49H$^+$ NK cells compared with Ly49H$^+$ WT NK cells on day 4 after MCMV infection (Fig. 6D, 6E). Thus, Crk proteins are required for the optimal effector functions, including IFN-γ production, activation, and proliferation, of Ly49H$^+$ NK cells during MCMV infection.

Discussion

In this study, we have demonstrated that Crk family proteins, including Crk and CrkL, are necessary for the optimal activation of Ly49H$^+$ NK cells during MCMV infection and for optimal phosphorylation of STAT4 and STAT1 during cytokine stimulation ex vivo. Naive *Crk*$^{-/-}$ and *CrkL*$^{-/-}$ dKO NK cells show defects in degranulation and IFN-γ production when assayed in vitro. Moreover, during MCMV infection, *Crk*$^{-/-}$ and *CrkL*$^{-/-}$ dKO Ly49H$^+$ NK cells showed an impaired ability to protect against primary MCMV infection. The diminished expansion of Ly49H$^+$ *Crk*$^{-/-}$ and *CrkL*$^{-/-}$ dKO NK cells during MCMV infection was not due to increased cell death or a general inability to divide.

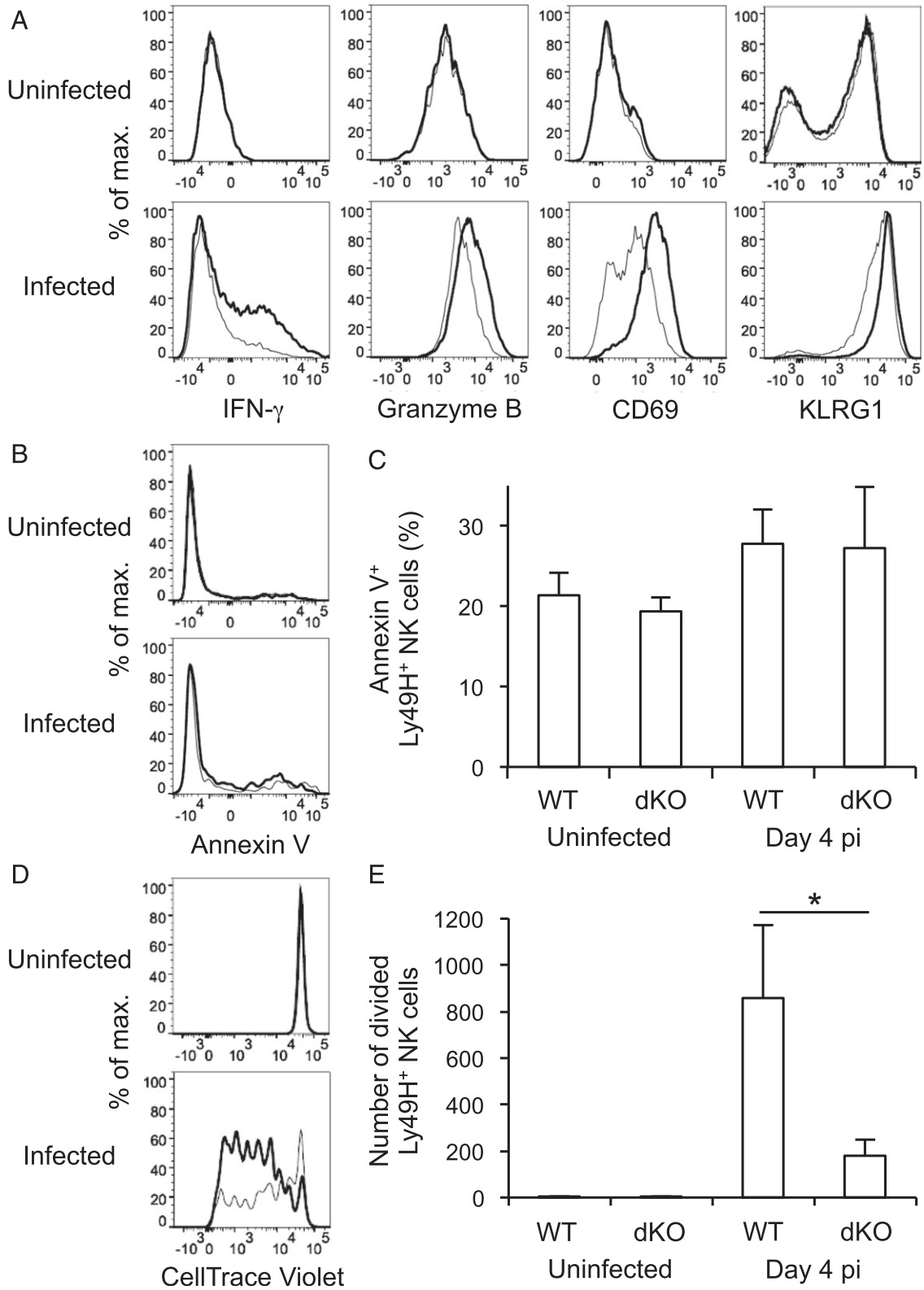

FIGURE 6. Crk proteins are required for optimal activation and IFN-γ^+ production of Ly49H$^+$ NK cells after MCMV infection. (**A**) Mixed BM chimeric mice were infected with 1×10^6 PFU MCMV. IFN-γ^+ production of WT (bold) and dKO (thin lines) Ly49H$^+$ NK cells was analyzed by intracellular staining on day 1.5 pi. CD69 and KLRG1 on WT (bold) and dKO (thin lines) Ly49H$^+$ NK cells were analyzed on days 1.5 and 7 pi, respectively. Data are representative of two to three experiments (n = 2–4 mice per experiment). (**B**–**E**) CellTrace Violet–labeled splenocytes (1.5×10^7) from BM chimeric mice were transferred into Ly49H-deficient mice and infected with 1×10^5 PFU MCMV. (B) Cell death of WT (bold) and dKO (thin lines) Ly49H$^+$ NK cells was analyzed by annexin V staining on day 4 pi. Data are representative of three experiments (n = 3–4 mice per experiment). (C) Percentages of annexin V$^+$ Ly49H$^+$ NK cells. Data were pooled from two experiments (n = 6 mice). (D) Cell divisions of WT (bold) and dKO (thin lines) Ly49H$^+$ NK cells were analyzed on day 4 pi. Data are representative of three experiments (n = 3–4 mice per experiment). (E) The number of divided Ly49H$^+$ NK cells was quantified. The number of divided Ly49H$^+$ NK cells was calculated by using the information on the number of splenocytes on day 4 pi, the percentages of donor NK cells, the percentages of Ly49H$^+$ NK cells, and the percentages of CellTrace Violet^{low} (non-undivided) NK cells. Data are representative of three experiments (n = 4 mice). *$p < 0.01$.

However, this defect in Ly49H$^+$ NK cell expansion in vivo correlated with the diminished phosphorylation of STAT4 in response to IL-12 and phosphorylation of STAT1 in response to IFN-α when tested ex vivo.

Consistent with studies examining the potential role of Crk in human NK cell function (6, 13, 14), dKO mouse NK cells exhibited defects in both cytotoxicity and cytokine production. Additionally, our results suggest that Crk proteins may play a role in the effector functions of both licensed and unlicensed NK cells. A recent study showed that the Abl-1 kinase, upstream of Crk (42, 43), is dispensable for NK cell inhibitory signaling and is not involved in mouse NK cell education (44). Similar frequencies of immature, intermediate, and mature NK cell subsets were observed in WT and Ncr1$^{iCre+/-}$ *Abl1*$^{fl/fl}$ C57BL/6 mice (44). In contrast, our results show that the frequency of mature dKO NK cells was slightly higher than WT NK cells in mixed BM chimeric mice. Although Crk and CrkL can be specific substrates for Abl kinase (45, 46), the functions of Abl and Crk in NK cells may be different, which might explain the variance in the frequency of mature NK cells between Crk x CrkL dKO mice and Ncr1$^{iCre+/-}$ *Abl1*$^{fl/fl}$ mice. Interestingly, Abl-1–deficient mouse NK cells displayed marginally enhanced effector responses after the triggering of the ITAM-coupled activating NK1.1R, which is reminiscent of studies showing that Crk phosphorylation was induced by the engagement of inhibitory KIR and CD94-NKG2AR in human NK cells (6, 12). Additionally, Abl kinases negatively regulate Crk activities during inhibition (12). In future studies, it will be of interest to investigate differences between Crk-deficient versus Abl-1–deficient NK cells during inhibitory signaling and NK cell education.

The molecular mechanisms underlying CMV-specific Ly49H$^+$ NK cell memory and cytokine-induced NK cell memory remain unclear. DAP12-mediated, ITAM-dependent signaling is important for the expansion and generation of memory Ly49H$^+$ NK cells (33), and IL-12 and type I IFNR signaling are essential for the optimal expansion and generation of memory Ly49H$^+$ NK cells during MCMV infection (33, 47, 48). Consistent with previous studies showing a critical role of STAT4 and STAT1 in regulating the response of mouse and human NK cells (40, 47–50), our results demonstrate that the levels of p-STAT4 or p-STAT1 in activated NK cells from dKO mice are reduced, which may explain the defects in cytokine production and degranulation by NK cells and the impaired expansion of NK cells during MCMV infection. Additionally, previous studies reported an IFN-dependent association of CrkL and Stat5 in human Daudi Burkitt's lymphoma cells treated with IFN-α and IFN-β (51). The complex of CrkL and Stat5 translocates to the nucleus and regulates gene transcription through DNA binding (51). In this study, we showed that the levels of p-STAT4 (in response to IL-12) or p-STAT1 (in response to IFN-α) in activated NK cells from dKO mice were reduced, compared with WT NK cells, which indicates that Crk family proteins may interact with Stat family proteins in NK cells. The exact molecular mechanisms will require further investigation.

In summary, in this study we demonstrate that Crk family proteins, including Crk and CrkL, are necessary for the optimal activation and proliferation of Ly49H$^+$ NK cells, potentially through modulating the phosphorylation of STAT4 and STAT1 during MCMV infection. Our findings reveal that Crk family proteins are essential for optimal NK cell–mediated host protection during infection.

Acknowledgments

We thank Dr. Marco Colonna (Department of Pathology and Immunology, Washington University School of Medicine, St. Louis, MO) for transferring NKp46-iCre mice to the laboratory of Dr. Dongfang Liu. We thank Dr. Yan Yang for critical reading of the manuscript. We thank Dr. Rongfu Wang and Dr. Changsheng Xing (Houston Methodist Research Institute) for providing reagents.

Disclosures

E.V. is a scholar of the Institut Universitaire de France and is cofounder of and a shareholder in Innate Pharma. The other authors have no financial conflicts of interest.

References

1. Lam, V. C., and L. L. Lanier. 2017. NK cells in host responses to viral infections. *Curr. Opin. Immunol.* 44: 43–51.
2. Morvan, M. G., and L. L. Lanier. 2016. NK cells and cancer: you can teach innate cells new tricks. *Nat. Rev. Cancer* 16: 7–19.
3. Bryceson, Y. T., and E. O. Long. 2008. Line of attack: NK cell specificity and integration of signals. *Curr. Opin. Immunol.* 20: 344–352.
4. Dustin, M. L., and E. O. Long. 2010. Cytotoxic immunological synapses. *Immunol. Rev.* 235: 24–34.
5. Liu, D., Y. T. Bryceson, T. Meckel, G. Vasiliver-Shamis, M. L. Dustin, and E. O. Long. 2009. Integrin-dependent organization and bidirectional vesicular traffic at cytotoxic immune synapses. *Immunity* 31: 99–109.
6. Liu, D., M. E. Peterson, and E. O. Long. 2012. The adaptor protein Crk controls activation and inhibition of natural killer cells. *Immunity* 36: 600–611.
7. Liu, D. 2014. The adaptor protein Crk in immune response. *Immunol. Cell Biol.* 92: 80–89.
8. Feller, S. M. 2001. Crk family adaptors-signalling complex formation and biological roles. *Oncogene* 20: 6348–6371.
9. Birge, R. B., C. Kalodimos, F. Inagaki, and S. Tanaka. 2009. Crk and CrkL adaptor proteins: networks for physiological and pathological signaling. *Cell Commun. Signal.* 7: 13.
10. Austgen, K., E. T. Johnson, T. J. Park, T. Curran, and S. A. Oakes. 2011. The adaptor protein CRK is a pro-apoptotic transducer of endoplasmic reticulum stress. *Nat. Cell Biol.* 14: 87–92.
11. Feller, S. M., B. Knudsen, and H. Hanafusa. 1994. c-Abl kinase regulates the protein binding activity of c-Crk. *EMBO J.* 13: 2341–2351.
12. Peterson, M. E., and E. O. Long. 2008. Inhibitory receptor signaling via tyrosine phosphorylation of the adaptor Crk. *Immunity* 29: 578–588.
13. Segovis, C. M., R. A. Schoon, C. J. Dick, L. P. Nacusi, P. J. Leibson, and D. D. Billadeau. 2009. PI3K links NKG2D signaling to a CrkL pathway involved in natural killer cell adhesion, polarity, and granule secretion. *J. Immunol.* 182: 6933–6942.
14. Zheng, P., L. M. Noroski, I. C. Hanson, Y. Chen, M. E. Lee, Y. Huang, M. X. Zhu, P. P. Banerjee, G. Makedonas, J. S. Orange, et al. 2015. Molecular mechanisms of functional natural killer deficiency in patients with partial DiGeorge syndrome. *J. Allergy Clin. Immunol.* 135: 1293–1302.
15. Sullivan, K. E., A. F. Jawad, P. Randall, D. A. Driscoll, B. S. Emanuel, D. M. McDonald-McGinn, and E. H. Zackai. 1998. Lack of correlation between impaired T cell production, immunodeficiency, and other phenotypic features in chromosome 22q11.2 deletion syndromes. *Clin. Immunol. Immunopathol.* 86: 141–146.
16. Davies, E. G. 2013. Immunodeficiency in DiGeorge syndrome and options for treating cases with complete athymia. *Front. Immunol.* 4: 322.
17. Maggadottir, S. M., and K. E. Sullivan. 2013. The diverse clinical features of chromosome 22q11.2 deletion syndrome (DiGeorge syndrome). *J. Allergy Clin. Immunol. Pract.* 1: 589–594.
18. McDonald-McGinn, D. M., and K. E. Sullivan. 2011. Chromosome 22q11.2 deletion syndrome (DiGeorge syndrome/velocardiofacial syndrome). *Medicine (Baltimore)* 90: 1–18.
19. Momma, K. 2010. Cardiovascular anomalies associated with chromosome 22q11.2 deletion syndrome. *Am. J. Cardiol.* 105: 1617–1624.
20. Jerome, L. A., and V. E. Papaioannou. 2001. DiGeorge syndrome phenotype in mice mutant for the T-box gene, Tbx1. *Nat. Genet.* 27: 286–291.
21. Guris, D. L., G. Duester, V. E. Papaioannou, and A. Imamoto. 2006. Dose-dependent interaction of Tbx1 and Crkl and locally aberrant RA signaling in a model of del22q11 syndrome. *Dev. Cell* 10: 81–92.
22. Guris, D. L., J. Fantes, D. Tara, B. J. Druker, and A. Imamoto. 2001. Mice lacking the homologue of the human 22q11.2 gene CRKL phenocopy neurocristopathies of DiGeorge syndrome. *Nat. Genet.* 27: 293–298.
23. Newbern, J., J. Zhong, R. S. Wickramasinghe, X. Li, Y. Wu, I. Samuels, N. Cherosky, J. C. Karlo, B. O'Loughlin, J. Wikenheiser, et al. 2008. Mouse and human phenotypes indicate a critical conserved role for ERK2 signaling in neural crest development. *Proc. Natl. Acad. Sci. USA* 105: 17115–17120.
24. Moon, A. M., D. L. Guris, J. H. Seo, L. Li, J. Hammond, A. Talbot, and A. Imamoto. 2006. Crkl deficiency disrupts Fgf8 signaling in a mouse model of 22q11 deletion syndromes. *Dev. Cell* 10: 71–80.
25. Giacomelli, M., R. Kumar, A. Soresina, N. Tamassia, T. Lorenzini, D. Moratto, S. Gasperini, M. Cassatella, A. Plebani, V. Lougaris, and R. Badolato. 2016. Reduction of CRKL expression in patients with partial DiGeorge syndrome is associated with impairment of T-cell functions. *J. Allergy Clin. Immunol.* 138: 229–240.e3.
26. Gennery, A. R. 2012. Immunological aspects of 22q11.2 deletion syndrome. *Cell. Mol. Life Sci.* 69: 17–27.

27. McLean-Tooke, A., D. Barge, G. P. Spickett, and A. R. Gennery. 2008. Immunologic defects in 22q11.2 deletion syndrome. *J. Allergy Clin. Immunol.* 122: 362–367, 367.e1–4.
28. Finocchi, A., S. Di Cesare, M. L. Romiti, C. Capponi, P. Rossi, R. Carsetti, and C. Cancrini. 2006. Humoral immune responses and CD27+ B cells in children with DiGeorge syndrome (22q11.2 deletion syndrome). *Pediatr. Allergy Immunol.* 17: 382–388.
29. Fodil-Cornu, N., S. H. Lee, S. Belanger, A. P. Makrigiannis, C. A. Biron, R. M. Buller, and S. M. Vidal. 2008. Ly49h-deficient C57BL/6 mice: a new mouse cytomegalovirus-susceptible model remains resistant to unrelated pathogens controlled by the NK gene complex. *J. Immunol.* 181: 6394–6405.
30. Narni-Mancinelli, E., J. Chaix, A. Fenis, Y. M. Kerdiles, N. Yessaad, A. Reynders, C. Gregoire, H. Luche, S. Ugolini, E. Tomasello, et al. 2011. Fate mapping analysis of lymphoid cells expressing the NKp46 cell surface receptor. *Proc. Natl. Acad. Sci. USA* 108: 18324–18329.
31. Park, T. J., K. Boyd, and T. Curran. 2006. Cardiovascular and craniofacial defects in Crk-null mice. *Mol. Cell Biol.* 26: 6272–6282.
32. Park, T. J., and T. Curran. 2008. Crk and Crk-like play essential overlapping roles downstream of disabled-1 in the Reelin pathway. *J. Neurosci.* 28: 13551–13562.
33. Sun, J. C., J. N. Beilke, and L. L. Lanier. 2009. Adaptive immune features of natural killer cells. [Published erratum appears in 2009 *Nature* 457: 1168.] *Nature* 457: 557–561.
34. Holl, E. K. 2013. Generation of bone marrow and fetal liver chimeric mice. *Methods Mol. Biol.* 1032: 315–321.
35. Shen, F. W., Y. Saga, G. Litman, G. Freeman, J. S. Tung, H. Cantor, and E. A. Boyse. 1985. Cloning of Ly-5 cDNA. *Proc. Natl. Acad. Sci. USA* 82: 7360–7363.
36. Nabekura, T., M. Kanaya, A. Shibuya, G. Fu, N. R. Gascoigne, and L. L. Lanier. 2014. Costimulatory molecule DNAM-1 is essential for optimal differentiation of memory natural killer cells during mouse cytomegalovirus infection. *Immunity* 40: 225–234.
37. Nabekura, T., and L. L. Lanier. 2014. Antigen-specific expansion and differentiation of natural killer cells by alloantigen stimulation. *J. Exp. Med.* 211: 2455–2465.
38. Vliegen, I., S. Herngreen, G. Grauls, C. Bruggeman, and F. Stassen. 2003. Improved detection and quantification of mouse cytomegalovirus by real-time PCR. *Virus Res.* 98: 17–25.
39. Nabekura, T., J. P. Girard, and L. L. Lanier. 2015. IL-33 receptor ST2 amplifies the expansion of NK cells and enhances host defense during mouse cytomegalovirus infection. *J. Immunol.* 194: 5948–5952.
40. Min-Oo, G., and L. L. Lanier. 2014. Cytomegalovirus generates long-lived antigen-specific NK cells with diminished bystander activation to heterologous infection. *J. Exp. Med.* 211: 2669–2680.
41. Bubić, I., M. Wagner, A. Krmpotić, T. Saulig, S. Kim, W. M. Yokoyama, S. Jonjić, and U. H. Koszinowski. 2004. Gain of virulence caused by loss of a gene in murine cytomegalovirus. *J. Virol.* 78: 7536–7544.
42. Feller, S. M., R. Ren, H. Hanafusa, and D. Baltimore. 1994. SH2 and SH3 domains as molecular adhesives: the interactions of Crk and Abl. *Trends Biochem. Sci.* 19: 453–458.
43. Raitano, A. B., Y. E. Whang, and C. L. Sawyers. 1997. Signal transduction by wild-type and leukemogenic Abl proteins. *Biochim. Biophys. Acta* 1333: F201–F216.
44. Ganesan, S., T. T. Luu, B. J. Chambers, S. Meinke, P. Brodin, E. Vivier, D. M. Wetzel, A. J. Koleske, N. Kadri, and P. Höglund. 2017. The Abl-1 kinase is dispensable for NK cell inhibitory signaling and is not involved in murine NK cell education. *Scand. J. Immunol.* 86: 135–142.
45. Anafi, M., M. K. Rosen, G. D. Gish, L. E. Kay, and T. Pawson. 1996. A potential SH3 domain-binding site in the Crk SH2 domain. *J. Biol. Chem.* 271: 21365–21374.
46. Oda, T., C. Heaney, J. R. Hagopian, K. Okuda, J. D. Griffin, and B. J. Druker. 1994. Crkl is the major tyrosine-phosphorylated protein in neutrophils from patients with chronic myelogenous leukemia. *J. Biol. Chem.* 269: 22925–22928.
47. Sun, J. C., S. Madera, N. A. Bezman, J. N. Beilke, M. H. Kaplan, and L. L. Lanier. 2012. Proinflammatory cytokine signaling required for the generation of natural killer cell memory. *J. Exp. Med.* 209: 947–954.
48. Madera, S., M. Rapp, M. A. Firth, J. N. Beilke, L. L. Lanier, and J. C. Sun. 2016. Type I IFN promotes NK cell expansion during viral infection by protecting NK cells against fratricide. *J. Exp. Med.* 213: 225–233.
49. Miyagi, T., M. P. Gil, X. Wang, J. Louten, W. M. Chu, and C. A. Biron. 2007. High basal STAT4 balanced by STAT1 induction to control type 1 interferon effects in natural killer cells. *J. Exp. Med.* 204: 2383–2396.
50. Simhadri, V. R., J. L. Mariano, O. Zenarruzabeitia, C. M. Seroogy, S. M. Holland, H. S. Kuehn, S. D. Rosenzweig, and F. Borrego. 2014. Intact IL-12 signaling is necessary for the generation of human natural killer cells with enhanced effector function after restimulation. *J. Allergy Clin. Immunol.* 134: 1190–1193.e1.
51. Fish, E. N., S. Uddin, M. Korkmaz, B. Majchrzak, B. J. Druker, and L. C. Platanias. 1999. Activation of a CrkL-stat5 signaling complex by type I interferons. *J. Biol. Chem.* 274: 571–573.

Supplementary Figure Legends:

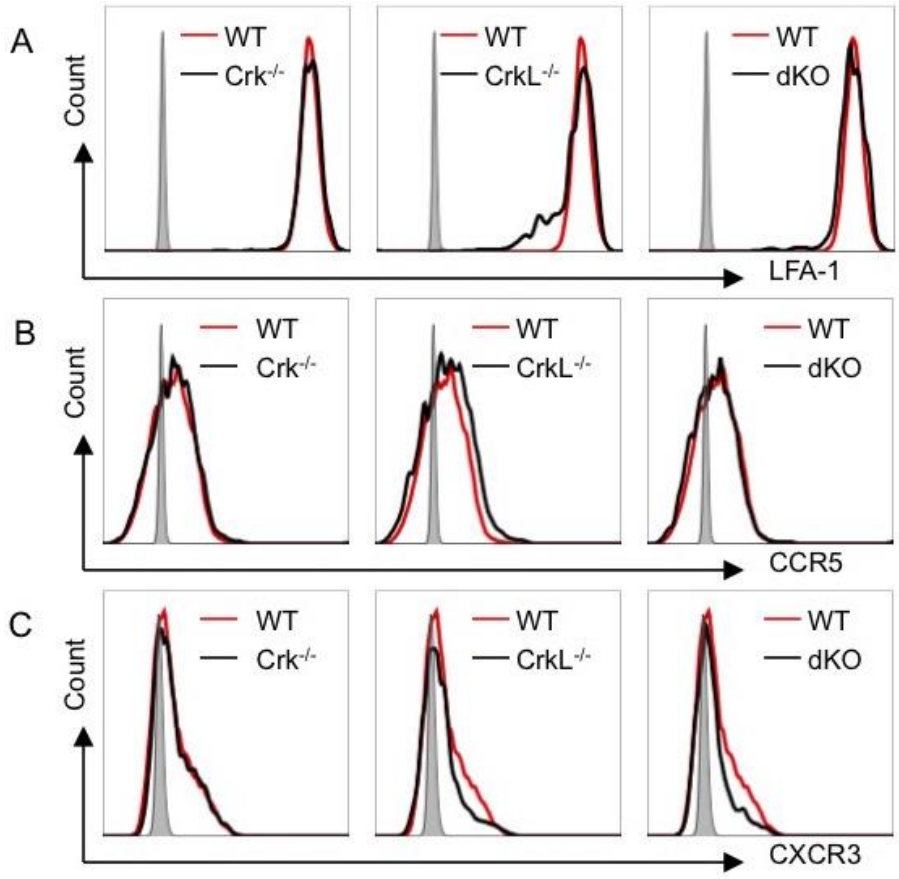

Supplemental Figure S1. Expression of LFA-1, CCR5, and CXCR3 molecules in NKp46-specific Crk-, CrkL-, and Crk- and CrkL-double deficient NK cells. (A) Expression of LFA-1 on NK cells from the spleens of NKp46-Crk-single-deficient ($Crk^{-/-}$), NKp46-CrkL-single-deficient ($CrkL^{-/-}$), and NKp46-Crk-CrkL-double-deficient (dKO) mice is shown. Expression of LFA-1 (stained with PE labeled anti-mouse CD11a/CD18 (LFA-1) mAb, Cat #141005, Biolegend) was compared between WT (red line) and KO (black line). (B) Expression of CCR5 (stained with CD195 (CCR5) mAb, Clone, HM-CCR5 (7A4), Cat #12195182, eBioscience™) and (C) Expression of CXCR3 (stained with CD183 (CXCR3) mAb, Clone, CXCR3-173, Cat #17183182, eBioscience™) on NK cells from the spleens of NKp46-Crk-single-deficient, NKp46-CrkL-single-deficient, and NKp46-Crk-CrkL-double-deficient mice were compared between WT (red line) and KO (black line). NK cells were gated on $NK1.1^{+}NKp46^{+}CD3^{-}$ lymphocytes. The isotype control staining (gray) is shown. Results are representative of three experiments.